Available online at www.sciencedirect.com
SCIENCE DIRECT®
Nuclear Instruments and Methods in Physics Research A 535 (2004) 324–329
NUCLEAR INSTRUMENTS & METHODS IN PHYSICS RESEARCH Section A
www.elsevier.com/locate/nima

GEM-based photon detector for RICH applications

Thomas Meinschad, Leszek Ropelewski*, Fabio Sauli

CERN, CH-1211 Geneva, Switzerland

Abstract

We describe the performance of a novel photon detector based on the Gas Electron Multiplier (GEM). With a CsI photocathode deposited on the first GEM in a cascade, the device permits to efficiently detect and localize single photoelectrons produced by UV photons between the CsI threshold (~6.2 eV) and the quartz window cutoff (~7.5 eV). The single-photon position accuracy achieved ~55 μm rms, and the excellent multi-photon resolution makes it well suited for Cherenkov ring imaging applications.

1. Introduction

Developed several years ago, the Gas Electron Multiplier (GEM) is a thin, metal-clad polymer foil perforated by a high density of holes, typically 50 per mm^2. On application of a potential difference between the two conducting sides, each hole acts as an individual proportional counter: electrons released in the upper gas volume drift into the channels and multiply in avalanche [1]. The resulting negative charge cloud transfers into the lower region, where it can be collected or further amplified; cascading several multiplying elements, one can reach very large gains. A unique feature of the device is that the multiplying electrodes are electrically separated from the readout plane; this guarantees protection of the sensitive electronics from accidental discharges, and permits freedom in the choice of the readout pattern, made with pads or strips of arbitrary shapes. Since only the electron component of the avalanche is detected, signals are very fast, typically 20–30 ns wide; the profile of induced charge, for a point-like ionization, has a FWHM of around 500 μm, resulting in good intrinsic multi-track resolution.

The excellent resolution and high-rate performance of multi-GEM devices has motivated their adoption as particle detectors for experiments operating in harsh radiation environments. The high-rate COMPASS spectrometer at CERN uses 20 triple-GEM detectors with an active area around 1000 cm^2 each and two-dimensional projective readout [2]. Many other GEM-based detectors are in use or under development in particle physics and other applied research fields [3].

The avalanche confinement in the holes results in efficient ion- and photon-mediated feedback

*Corresponding author.
E-mail address: leszek.ropelewski@cern.ch (L. Ropelewski).

0168-9002/$ - see front matter © 2004 Elsevier B.V. All rights reserved.
doi:10.1016/j.nima.2004.07.277

suppression and permits to attain very large gains even in pure noble gases and their mixtures [4]. Multi-GEM devices are capable to detect and localize single electrons emitted by an internal photocathode; particularly suitable are CH_4 and CF_4 gas fillings, in which quantum efficiencies close to vacuum have been obtained, and secondary photon-mediated processes are minimal [5,6]. Recently, sealed small-size GEM detectors with alkali photocathodes have been manufactured and tested, a first attempt toward the realization of large area gas devices capable of detecting and localizing photons at visible wavelengths [7].

In the early works, the photosensitive material was deposited on the inner side of the photon entrance window (the so-called transmissive photocathode); an attractive option is to deposit a reflective photocathode on the upper GEM electrode, facing the window [8,9]. The high-surface field escaping from the GEM holes permits to efficiently extract photoelectrons and to inject them into the cascade of multipliers; a zero or reverse field in the drift region minimizes the contribution of direct ionization in the gap (Fig. 1). The strong suppression of photon and ion feedback in this configuration results in efficient single photon detection and extended lifetime of the detector.

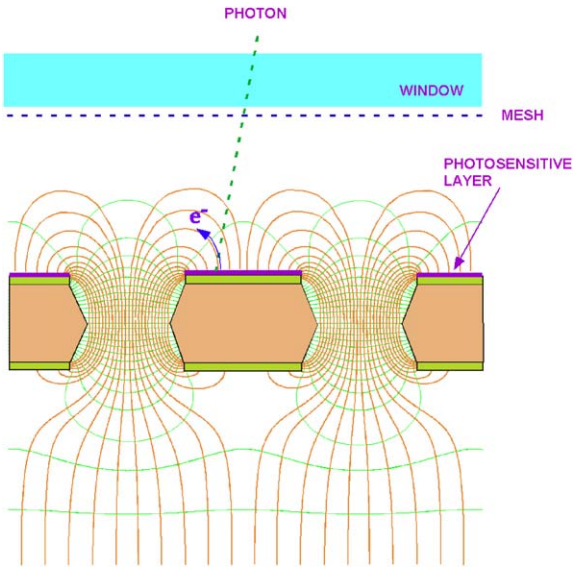

Fig. 1. Schematics and fields of the reflective photocathode GEM.

2. Experimental setup

In view of applications of the technology to Cherenkov ring imaging, we have investigated the single-photon localization properties of a medium-size triple-GEM detector with the reflective photocathode geometry. The detector structure has been described in previous work; it consists essentially of a clean box containing all active electrodes, externally powered [10]. The triple-GEM device has an active area of $10 \times 10\,cm^2$, and projective strip readout on the anode; the first GEM electrode, facing the window, was coated on one side with a thin layer of CsI using the vacuum evaporation setup developed at CERN. Transfer and induction gaps in the detector are 2 mm thick, with a 3 mm thick drift region. A 5 cm diameter UV quality quartz window, mounted on one side of the box, allows exposure of the central part of the detector to UV photons; the upper drift electrode is made with a thin mesh having 90% optical transparency. Several thin polymer-covered openings permit exposure to X-rays for calibration purposes. To obtain the best performance, the copper electrodes of the CsI-coated GEM foil have been gold-plated. Although we could not verify directly the quantum efficiency of the layer, the workshop has a large experience in consistently producing large area devices used, for the COMPASS RICH [11]. The electrodes have to be briefly handled in air, but all care was taken to avoid prolonged exposure.

The detector assembly, that involves time-consuming manipulations, is done in a nitrogen-filled glove box. After completion, the detector is quickly transferred to the experimental setup and flushed with the operating gas, and mounted on an optical bench supporting the photon source and the collimators; a micrometer permits to accurately displace the chamber in front of the collimated beam for position and linearity measurements.

As photon source, we have used the relaxation discharges in a sealed glass vessel containing

low-pressure hydrogen; energy and frequency of the discharges are controlled by external circuitry. A capacitive pickup on the lamp provides the discharge time, used for measurements in coincidence; a collimator in front of the detector controls the size of the beam, and a set of fine wire meshes with moderate optical transparency permits to modulate its intensity. Charge signals are recorded on eight adjacent readout strips, at 200 μm pitch, using low-noise amplifiers followed by gated charge ADCs; linearity of response and uniformity of gain are calibrated using the X-ray source.

As filling gas, we have used a mixture of argon and methane or pure methane, transparent to photons of energy, between the CsI quantum efficiency threshold (~6.2 eV) and the window cutoff (~7.5 eV). The former choice has the potential advantage of requiring a lower operating voltage, although one can expect a small decrease in quantum efficiency due to backscattering of the photoelectrons by the noble gas molecules [12]. Confirming, however, an earlier study [13], we have observed, after the main photon signal, delayed pulses consistent with the hypothesis of being due to ion feedback. This point requires further investigation. All results discussed in this paper have been obtained in pure CH_4, where such delayed pulses are not observed; higher voltages are, however, needed. Powered with a standard resistive divider, the detector was operated with equal voltages across the three GEMs (515 V) and fields in the transfer and induction gaps (~4.6 kV/cm); for UV photon detection, the drift potential was kept equal or slightly lower than the one applied to the photocathode (the upper GEM electrode).

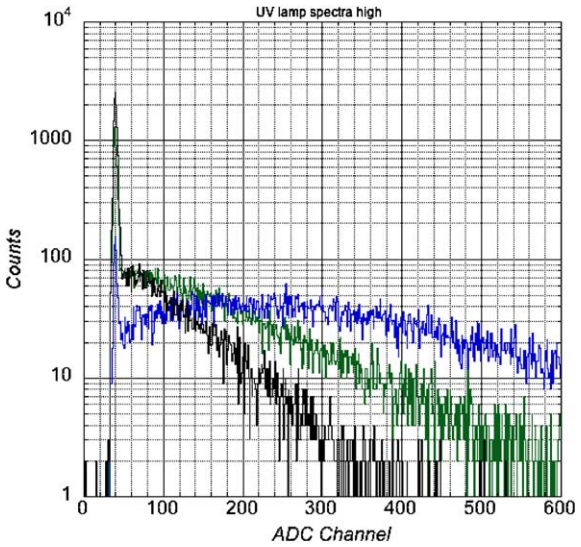

Fig. 2. Detected charge distributions at decreasing UV light intensity.

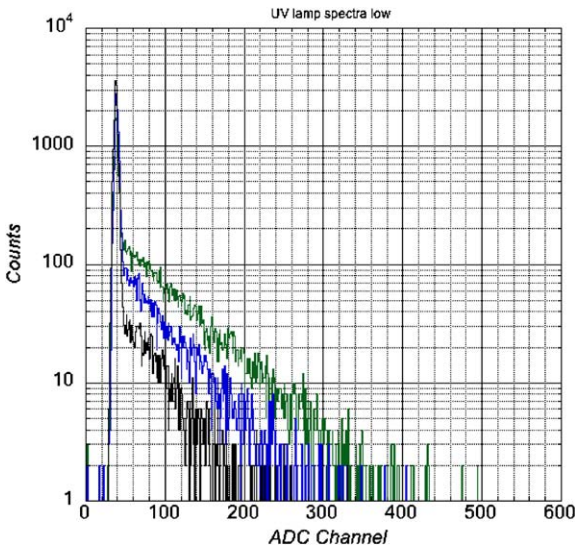

Fig. 3. Detected charge distributions in the single photoelectron region.

3. Results

Figs. 2 and 3 show pulse height spectra obtained by progressively reducing the UV source intensity, recorded at constant detector gain and equal number of coincidence signals from the lamp. One can clearly notice the transition from multiple photon detection (the broader rightmost spectrum in Fig. 2) to single photon counting, demonstrated by the reduction in integral count with an identical shape of the spectra in Fig. 3; as expected, the photon have an exponentially decreasing shape. The integrated counts in the exponential divided by the number of triggers provides the probability of detecting one or more photoelectrons; assuming

a Poisson distribution, an integrated probability around 30% (lower curve in Fig. 3) guarantees that most events correspond to a single photoelectron.

The charge profile recorded for a typical event is shown in Fig. 4; it has a FWHM of 600 μm, mostly determined by diffusion and avalanche fluctuations of the charge propagating through the multipliers and transfer regions. Fig. 5 provides the experimental distribution of the cluster size for single electron avalanches. Because of the limited region equipped with electronics (8 strips, or 3.2 mm) we could not directly study the two-photon resolution, but the width of the distribution suggests that simple software should disentangle two hits about 1 mm apart, an essential feature in view of RICH applications.

In the present work, one set of parallel strips was used to record the charge profiles. Collimating the photon beam of an estimated width of 100 μm, and displacing the micrometer with the detector in the direction perpendicular to the strips, we have recorded around one thousand events per position and computed the corresponding center of gravity distribution. Fig. 6 shows the correlation between the geometrical position and the computed center of gravity. The full range of the scan is limited to about half a mm, to avoid distortions arising if part of the charge profile exceeds the instrumented region; within this range, the correlation is linear, as shown by the fit. The distribution of the center

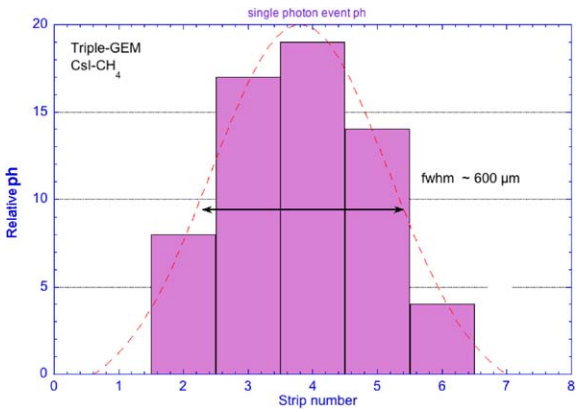

Fig. 4. Charge profile for a single electron avalanche. The strip width is 200 μm.

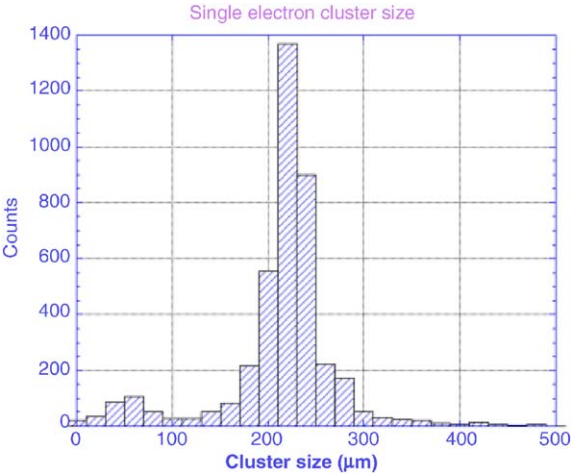

Fig. 5. Cluster charge width (rms) for single electron avalanches.

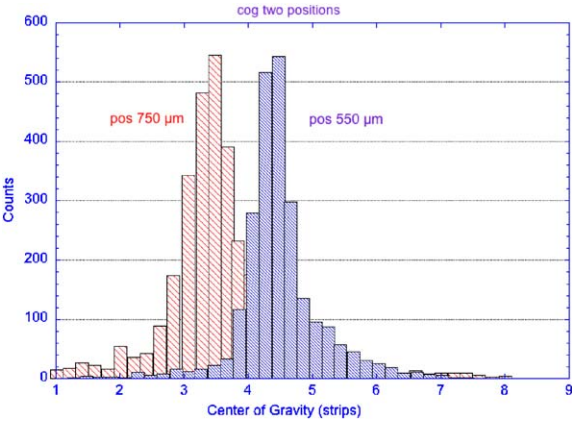

Fig. 6. Distribution of computed center of gravity for two positions of the collimated photon source.

of gravity, recorded for two positions 200 μm apart, is shown in Fig. 7, and has a FWHM of 160 μm. Subtracting the estimated source width (100 μm) we can infer an intrinsic single photon localization accuracy around 125 μm FWHM (~55 μm rms).

Two-dimensional projective readout can be obtained using a double layer board, as shown in the previous work; the excellent correlation between the charge recorded on the two projections can be used to resolve the ambiguities arising in multi-hit events [14]. This method should be

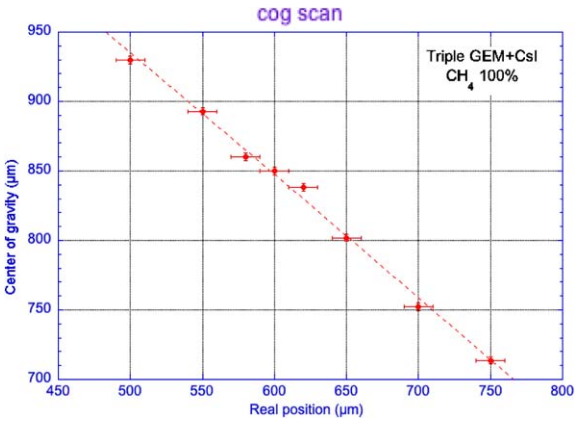

Fig. 7. Correlation between real and computed position of the collimated source.

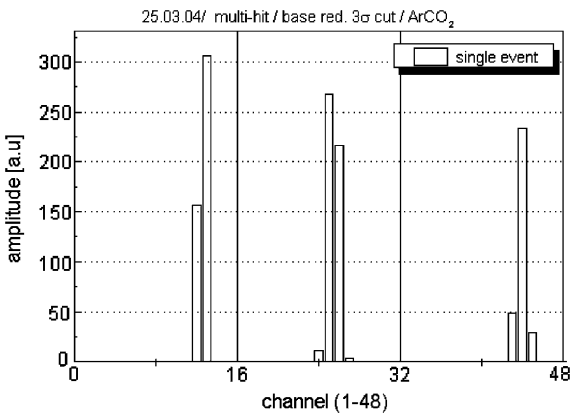

Fig. 8. A single photoelectron event recorded with the hexaboard readout.

even more powerful for the wide charge distributions as those produced by single electrons, and will probably allow to resolve the ambiguities arising in recording not too populated Cherenkov rings.

The ultimate resolution of a GEM detector can be achieved using as pickup electrode a matrix of pads, with a size corresponding to the intrinsic width of the detected avalanche charge (a few hundred microns in optimal conditions); this is, however, a very expensive proposition. An elegant alternative, offering performances in between projective strips and pixel readouts has been developed under the name "hexaboard"; it consists of a matrix of charge collecting hexagonal pixels, covering the readout plane, and interconnected on the backside in rows along three directions at 120 to each other [15]. For each event, three independent charge profiles are recorded, providing an ambiguity-free reconstruction up to large hit multiplicities. With a typical pad size of around 500 μm, and thanks to the charge spread in multi-GEM structures, a signal is collected on several adjacent strips in each projection permitting accurate positioning. At the time of this writing, we had started the operation of a GEM-CsI RICH prototype with hexaboard readout; the detector has an hexagonal active area, with 170 readout channels on each of the three projections, each channel providing the signal from a row of interconnected hexagonal pads at a pitch of 520 μm. Fig. 8 shows as an example the charge recorded along the three projections for a single electron avalanche. The data analysis, now in progress, aims at determining the position accuracy, two-photon separation and multi-photon resolution power of the device. A large detector using the hexaboard concept is in construction for the experiment MICE [16].

Acknowledgements

We would like to acknowledge the dedicated help of Rui de Oliveira (CERN-TS-DEM) for manufacturing the GEM foils, Miranda van Stenis (CERN-PH-TA1) for the construction of the detector, André Braem (CERN-PH-TA1) for the CsI deposition, and Luciano Musa (CERN-PH-ED) for the procurement of the electronics used in part of the measurements.

References

[1] F. Sauli, Nucl. Instr. and Meth. A 386 (1997) 531.
[2] C. Altunbas, et al., Nucl. Instr. and Meth. A 490 (2002) 177.
[3] F. Sauli, Nucl. Instr. and Meth. in Phys. Res. A 522 (2004) 93.
[4] A. Buzulutskov, et al., Nucl. Instr. and Meth. A 433 (1999) 471.
[5] B.K. Singh, et al., Nucl. Instr. and Meth. in Phys. Res. A 454 (2000) 364.

[6] A. Breskin, et al., Nucl. Instr. and Meth. in Phys. Res. A 483 (2002) 670.
[7] D. Mörmann, et al., Nucl. Instr. and Meth. A 504 (2003) 93.
[8] R. Bouclier, et al., IEEE Trans. Nucl. Sci. NS-44 (1997) 646.
[9] D. Mörmann, et al., Nucl. Instr. and Meth. A 478 (2002) 230.
[10] A. Bressan, et al., Nucl. Instr. and Meth. A 425 (1999) 262.
[11] E. Albrecht, et al., Nucl. Instr. and Meth. in Phys. Res. A 502 (2003) 112.
[12] A.D. Mauro, et al., Nucl. Instr. and Meth. in Phys. Res. A 371 (1996) 137.
[13] A. Buzulutskov, et al., Nucl. Instr. and Meth. A 442 (2000) 68.
[14] A. Bressan, et al., Nucl. Instr. and Meth. A 425 (1999) 254.
[15] S. Bachmann, et al., Nucl. Instr. and Meth. A 478 (2002) 104.
[16] V. Ableev, et al., Nucl. Instr. and Meth. in Phys. Res. A 518 (2004) 113.